

## HEAVY METAL IONS IN POLLUTED WATER REMOVABLE BY SYNTHESISING A NEW COMPOUNDS FOR DITHIOCARBAMATE DERIVATIVES

Aeed S. Al-fahdawi<sup>1\*</sup>, Shaaban K. Mohamed<sup>2</sup>, Herman Potgeiter<sup>3</sup> and Abdullatif Alfutimie<sup>4</sup>

<sup>1</sup>Department of Chemistry, College of Education for Girls, University of Anbar, Iraq

<sup>2,3</sup>Chemistry and Environmental Division, Manchester Metropolitan University, UK

<sup>4</sup>Department of Chemical Engineering, University of Manchester, Manchester, UK

(Received December 11, 2023; Revised June 14, 2024; Accepted June 17, 2024)

**ABSTRACT.** Metal ion poisoning in water and industrial effluents threatens ecosystems and human health. The development of efficient metal ion removal technologies has garnered attention in recent years. This work synthesizes and characterizes dithiocarbamate complexes as metal ion scavengers. Used to make dithiocarbamate ligands. Different metal salts were added to carbon disulfide and the proper amines to initiate substitution reactions. The complexes were characterized using FTIR, UV-Vis, mass spectroscopy, <sup>13</sup>C-, <sup>1</sup>H-NMR, magnetic susceptibility, melting point, and electrical conductivity molar EC. Data from spectroscopy and analysis indicate the development of two-type macrocyclic complexes with the formula [M(L)]<sub>2</sub>, where M = Fe<sup>II</sup>, Co<sup>II</sup>, and Zn<sup>II</sup> ions. Tetrahedral geometries around the metal core and the second general formula [M(L)(H<sub>2</sub>O)<sub>2</sub>]<sub>2</sub>, where M = Mn<sup>II</sup>, Ni<sup>II</sup>, Cu<sup>II</sup>, suggested octahedral structures. Heavy water pollution has been removed using this essential ligand. Metal ion scavenging of 96–98% was possible with the produced dithiocarbamate complexes. This work developed unique and efficient strategies for metal contamination removal from aquatic settings, promising environmental remediation and human health protection. Optimizing synthesis conditions and scaling up operations are needed to fully use these compounds in real-world applications.

**KEY WORDS:** Dithiocarbamate ligand, Transition metal complexes, Spectral characterization, Coordination chemistry, Dithiocarbamate complexes, Scavenger heavy metal ions

### INTRODUCTION

Scavenging metal ions by the use of dithiocarbamate complexes has garnered a lot of interest in recent years owing to the fact that it has the potential to be used in a variety of disciplines, such as environmental remediation, wastewater treatment, and metal recovery. Metal ions, including heavy metals, are recognized to provide major dangers to both human health and the environment when they are present in large quantities. In light of this, there is an immediate need for technologies that are both effective and kind to the environment for the removal of these metal ions [1]. Dithiocarbamate ligands may be found in at least nine distinct coordination modes, resulting in the creation of a diverse array of geometries. The structural variations mostly arise from the substitution control exerted on the nitrogen atom of the dithiocarbamate group. The morpholinyl dithiocarbamate ligand responds with metal ions (Ni<sup>II</sup>, Cu<sup>II</sup>, and Zn<sup>II</sup>) to generate thiocarbamate complexes [2]. This procedure yielded dithiocarbamate chemicals. Cu<sup>II</sup> dithiocarbamate molecules were manufactured using N-butyl-N-phenyl dithiocarbamate ([Cu(L<sub>1</sub>)<sub>2</sub>]) and N-ethyl-N-ethanol dithiocarbamate ([Cu(L<sub>2</sub>)<sub>2</sub>]). The determination of this study was to catch a profounder understanding of the compound structural characteristics under different conditions [3]. The researchers exposed that complexes of di-isobutyl-dithiocarbamate (M(S<sub>2</sub>CNiBu<sub>2</sub>)<sub>n</sub>) serve as precursors to ternary sulfides. The sulfides contain of Fe-Ni, Fe-Cu, and Ni-Co. In addition, the compounds contained of both complexes [4]. Many pharmaceutical companies used organogold compounds to produce antibacterial drugs. This work inspected the structure and properties of a cyclometallated Au(III) dithiocarbamate complex that has potential

\*Corresponding authors. E-mail: [edw.aeedchemistry@uoanbar.edu.iq](mailto:edw.aeedchemistry@uoanbar.edu.iq)

This work is licensed under the Creative Commons Attribution 4.0 International License

therapeutic applications [5]. Pt-(phenanthroline) (tertaryl dithiocarbamate) is prepared using these compounds. The subject of this discussion will be pharmacology. The chemical which consists of 1,10-phenanthroline (phen) and tertaryl-dithiocarbamate, was prepared. The compound was analyzed using UV-Vis, FT-IR,  $^1\text{H}$  NMR, and  $^{13}\text{C}$  NMR techniques. This study investigated the distinctive characteristics of a platinum compound in order to ascertain its properties [6]. During this process, dithiocarbamate-sugar compounds have similar effects to TB medicines [7]. The dithiocarbamate moiety's usage in agriculture as an antibacterial and antiviral agent [8].

## EXPERIMENTAL

### Materials

Ethylene diamine, *m*-hydroxybenzaldehyde, ethanol, hydrogen bromide, methanol, sodium borohydride, potassium hydroxide, carbon disulfide, and dimethyl sulfoxide were used.

### Instrumentation

The prepared compounds were identified by melting points of all synthesized compounds were recorded on an Electro thermal DMP-500 melting-point device. FTIR was measured using Shimadzu (FTIR)–8400S spectrophotometer in the  $4000\text{--}200\text{ cm}^{-1}$  spectrum range. Spectra were performed as CsI and KBr discs. The electronic spectra for the ligand and its complexes were determined on a UV-Visible JASCO-V-650 device spectrophotometer, in DMSO solutions with  $10^{-3}$  M. concentration.  $^1\text{H}$ - and  $^{13}\text{C}$ - NMR spectra were recorded on Bruker 400MHz SWISS.TS AG using DMSO and  $\text{CDCl}_3$  as solvents. The metal content of the complexes was examined using a Nov (A.A.) 350 atomic absorption spectrophotometer. A magnetic susceptibility balance (Sherwood Scientific) was used to measure magnetic moments.

### Preparation

*Preparation of the Schiff Base and secondary amine* [9, 10]. The chemical Schiff base was synthesized by combining 1.98 g (16.70 mmol) of *m*-hydroxybenzaldehyde with continuous stirring to 0.5 g (8.31 mmol) of ethylene diamine dissolved in 40 mL of ethanol. Subsequently, 3-4 drops of HBr acid were added to the solution. After 3 hours of stirring, the precipitate was collected, filtered, rinsed with solvent, and dried under vacuum pressure. This process yielded a yellow-colored chemical weighing 1.59 g, which corresponds to a yield of 71.62%. The melting point was 206-208 °C.

The preparation of the secondary amine obtained by dissolving 0.75 g (2.79 mmol) of Schiff base, which had been synthesized earlier, in 40 mL of a combination of dichloromethane and methanol at a ratio of 1:3 resulted in the preparation of the compound secondary amine. With each successive addition, 0.51 g (13.48 mmol) of  $\text{NaBH}_4$  was added to the solution. After that, the combination was allowed to sit undisturbed for a period of twelve hours. Through the addition of water and dichloromethane to the solution, the organic layer was successfully separated. After being rinsed with water four times at a ratio of four times fifty milliliters, the organic layer was dried with magnesium sulfate. After filtering and evaporating the solution under vacuum pressure, a white precipitate with a purity of 83.22% and a temperature range of 175–176 °C was obtained.

*Ligand preparation.* The ligand [L] was synthesized by dissolving 0.369 g (1.47 mmol) of the previously obtained secondary amine in 35 mL of ethanol. Then, 0.164 g (2.54 mmol) of KOH dissolved in 3 mL of ethanol was added to the mixture with continuous stirring. The concoction was maintained in a frigid bath. After a duration of 15 min, a volume of 0.44 mL (equivalent to 7.28 mmol) of  $\text{CS}_2$  was introduced into the solution, which was then subjected to stirring for a

period of two hours. Filtration was used to gather the potassium dithiocarbamate salt. Subsequently, it underwent a washing process using 5 mL of methanol (MeOH) and 10 mL of ether. Afterward, it was subjected to vacuum drying, resulting in a yield of 0.55 g (75.34%) and a melting point range of 190–192 °C.

*The general method for preparing a macrocyclic complexes [11].* In order to create the complexes, one mole of potassium dithiocarbamate salt (KDTC) is used as a ligand, and one mole of the metal salt is utilized as the central ion.  $Mn^{II}$ ,  $Fe^{II}$ ,  $Co^{II}$ ,  $Ni^{II}$ ,  $Cu^{II}$ , and  $Zn^{II}$  are the six metals that are used in the process of producing the macrocyclic complexes. In order to finish the precipitation process, the combination that contains the ligand salt, the metal, and its solvents is agitated for three hours. When adding distilled water, it is done so only when it is absolutely essential. In the process of filtering, washing with the solvent, and drying the precipitate, a macrocyclic complex is produced. The color of this complex varies depending on the kind of metal that is being used. The complexes (I)  $[Mn(L)(H_2O)_2]$  given deep brown color, 67.10%, and over 300 °C; (II)  $[Fe(L)]_2$  given deep red color, 65.68% and 280 °C decomposed; (III)  $[Co(L)]_2$  given deep green, 77.63% and m.p. over 300 °C; (IV)  $[Ni(L)(H_2O)_2]$  given green color, 71.06% and 197-199 °C; (V)  $[Cu(L)(H_2O)_2]$  given Deep red color, 84.41% and 190-192°C; (VI)  $[Zn(L)]_2$  given white color, 62.33% and 200-202 °C.

#### *The efficiency of ligands in ecosystems*

The ligand was used for the purpose of removing heavy element ions from contaminated settings, particularly in industrial waste water, where these ligands are responsible for removing heavy metals from waste environments. Because of the presence of enterprises that create water that is contaminated with  $Fe^{II}$  and  $Cu^{II}$ , we are dependent on two ions, namely iron and copper. These companies are involved in the copper and iron industries.

#### *Sample preparation for the contaminated water*

A sample of industrial wastewater was collected from the State Company for Copper, Iron, and Plastic Industries (Amiriyat Al-Fallujah) in Iraq. The sample was sent to the laboratory for the purpose of quantifying heavy metals using atomic absorption technology (A.A.). The measurement of these components was conducted using atomic absorption spectrometry at the Market Research and Consumer Protection Center at the University of Baghdad. Upon concluding the measurements, the concentration of iron was determined to be 30.4440 mg/L, whereas the concentration of copper was discovered to be 5.5479 mg/L.

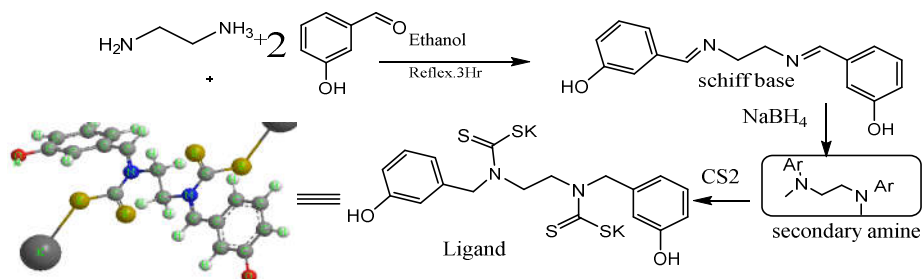
#### *Retrieval of heavy metal Ions by the prepared ligand [12]*

The pre-made ligand (0.10 g, 0.2 mmol) was combined with 5 mL of pure ethanol. Subsequently, the solution was introduced gradually into 30 mL of water containing heavy metals, creating a mildly alkaline environment. The solution was produced as a solid that settled at the bottom of the beaker. The filtrate was subjected to filtration and then re-measured using atomic absorption spectroscopy (A.A.) to determine the concentrations of the remaining contaminated substances. The concentrations of iron (Fe) and copper (Cu) were found to be 0.4139 mg/L and 0.1897 mg/L, respectively. The elimination efficiency was 98% for Fe and 96% for Cu, as shown by the following equation:  $E(\%) = [(C_0 - C_e)/C_0] \times 100$ .

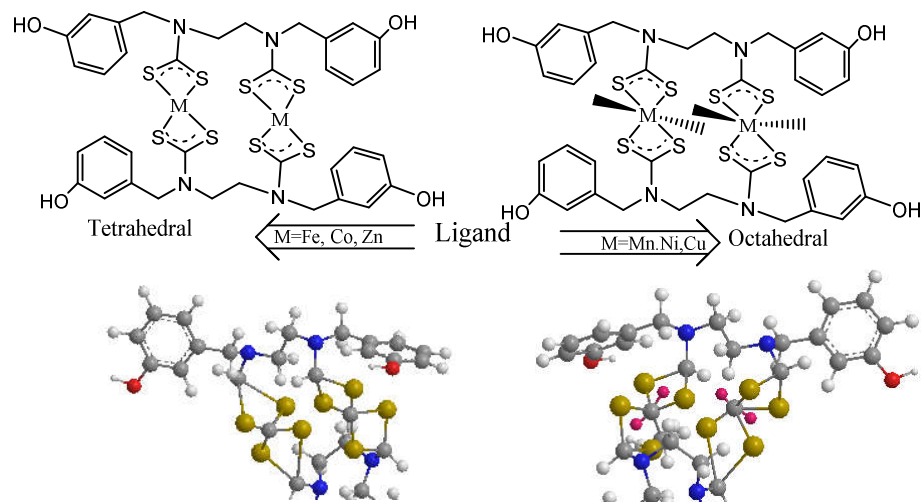
The variable  $E(\%)$  indicates the capture percentage,  $C_0$  denotes the beginning concentration of iron or copper ions, and  $C_e$  represents the end concentration of iron or copper ions.

## RESULTS AND DISCUSSION

The synthesis of organic molecules, namely Schiff bases, was achieved by reacting primary amines (ethylene diamine) with *m*-hydroxybenzaldehyde in the presence of ethanol. The Schiff base compound was dissolved in methanol and then reacted with NaBH<sub>4</sub> to yield the secondary amine. The ligand salt was formed by adding carbon disulfide (CS<sub>2</sub>) and potassium hydroxide (KOH) to the dissolved secondary amine. A satisfactory amount of the ligand salt was obtained by reacting a secondary amine with carbon disulfide (CS<sub>2</sub>) in the presence of KOH (Scheme 1).



Scheme 1. The preparation of ligand and its structure.



Scheme 2. The preparation of cyclic complexes.

As a result of the reaction between the ligand salt and metal chloride in a ratio of one to one, the complexes were effectively produced. In this approach, the metal ion played a crucial role in the self-assembly of binuclear cyclic complexes, which resulted in the formation of two general formulae which were tetrahedral and octahedral respectively. There is one atom in the center of the tetrahedral structure, and there are four atoms on the five sides. By forming bond angles of 109.5° with each of the surrounding atoms, the center atom forms bonds with each of the surrounding atoms. Octahedral bond angle values of 90° and 180° are what distinguish the

octahedral form from other shapes. The angle that exists between any of the four atoms that make up the square base of the two pyramids in the octahedral structure is  $90^\circ$ , and the angle that exists between any of those atoms and any of the vertex atoms is also  $90^\circ$ . The values and structures of angles are consistent with these theoretical values for angles, which are in accord with the values. This is shown in Schemes 1 and 2.

#### IR spectrum

The FTIR spectrum of the Schiff-base is compared to the FTIR spectra of the main amine (ethane-1,2-diamine) and *m*-hydroxybenzaldehyde the starting ingredients. The FTIR spectrum of the Schiff-base does not exhibit a band at  $1700\text{ cm}^{-1}$  that may be attributed to  $\nu(\text{C}=\text{O})$  stretching, in contrast to the spectrum seen in the *m*-hydroxybenzaldehyde spectrum. Contrary to ethane-1,2-diamine, the spectra exhibit no peak at  $3390\text{ cm}^{-1}$  as a result of the stretching of the  $\nu(\text{NH}_2)$  group. Nevertheless, the spectra exhibited a distinct band. The presence of the  $\nu(\text{C}-\text{H})$  aromatic stretching vibration at a wavenumber of  $3059\text{ cm}^{-1}$  is confirmed. The spectra exhibited two well defined peaks, suggesting the presence of aldehydic  $\nu(\text{C}-\text{H})$  bonds with greater lengths. The peaks attained their highest levels at  $2870\text{--}2818\text{ cm}^{-1}$ . Band detected at  $2731\text{ cm}^{-1}$  is referred to  $\nu(\text{C}-\text{H})$  stretching of the aldehydic moiety. The spectrum recorded bands at  $1615$  and  $1076\text{ cm}^{-1}$  assigned to  $\nu(\text{C}=\text{N})$  and  $\nu(\text{C}-\text{N})$ , respectively. The appearance of  $(\text{C}=\text{N})$  imine band and the disappearance of the amine  $(\text{NH}_2)$  band in the spectrum confirmed the formation of the Schiff base [14]. Band at  $1585\text{ cm}^{-1}$  is referred to  $\nu(\text{C}=\text{C})$  aromatic stretching. The FTIR spectra of the secondary amine compounds shows prominent bands related to the formation of secondary amine. The appearance of the amine  $(\text{N}-\text{H})$  band in the spectrum confirmed the formation of secondary amine [14]. The spectrum shows no band around  $1635\text{ cm}^{-1}$  that may be assigned to  $\nu(\text{C}=\text{N})$  stretching compared with that reported in Schiff-base spectrum. Further, the spectrum shows band around  $3286\text{ cm}^{-1}$  which could be related to  $\nu(\text{N}-\text{H})$  band in the spectrum confirmed the formation of the secondary amine [15]. The FTIR spectrum of ligand is compared with the FTIR spectrum of the secondary amine. The spectrum of L shows no band around  $3390\text{ cm}^{-1}$  which could be related to  $\nu(\text{N}-\text{H})$  stretching, compared with that observed in the secondary amine spectrum. The spectrum shows a band at  $3367.71\text{ cm}^{-1}$  which corresponds to  $\nu(\text{O}-\text{H})$  [16]. Moreover, the new band at  $1454\text{ cm}^{-1}$  is assigned to  $\nu(\text{C}-\text{N})$  stretching of  $(\text{N}-\text{CS}_2)$  moiety. The FTIR spectrum reveals two new bands at  $1126$  and  $1087\text{ cm}^{-1}$  attributed to  $\nu_{\text{as}}(\text{CS}_2)$  and  $\nu_{\text{s}}(\text{CS}_2)$  of carbon disulphide [17], respectively. Fourier transform infrared spectra are detected the coordination shape of dithiocarbamate metal complexes. To identify the appropriate regions for spectra, observe the bands at  $400\text{--}460$ ,  $950\text{--}1190$ , and  $1450\text{--}1500\text{ cm}^{-1}$ . The M-S bond vibration is also associated with bands in the range of  $400\text{--}460\text{ cm}^{-1}$  [18]. The  $\nu_{\text{as,s}}(\text{CS}_2)$  vibration is characterized by its stretching frequencies, which distance from  $950$  to  $1190\text{ cm}^{-1}$ . The third area, ranging from  $1450$  to  $1500\text{ cm}^{-1}$ , corresponds to the  $\nu(\text{C}-\text{N})$  vibration of the  $\nu(\text{N}-\text{CS}_2)$  band [18]. The occurrence of a band at around  $1500\text{ cm}^{-1}$  is anticipated to originate from a polar structure, such as  $(^-\text{N}=\text{CSS}^2)$ , as stated in reference [19]. The alkyl group's growing electron-donating nature would stabilize this structure and raise the  $\nu(\text{C}-\text{N})$  wave number. The other bands are obsolete and included in Table 1.

#### Mass spectrometry

*Mass spectrum of Schiff base.* The electrospray (+) mass spectrum of Schiff base revealed the presence of the parent ion peak (M)<sup>+</sup>, which was  $(\text{C}_{16}\text{H}_{16}\text{N}_2\text{O}_2)$  and belonged to the basic molecular ion. This peak was located at  $m/z = 268$ . It is necessary, in addition to other pieces, that  $m/z = 236$  belonged to  $\text{C}_{16}\text{H}_{16}\text{N}_2$ ,  $m/z = 148$  belonged to  $\text{C}_9\text{H}_{12}\text{N}_2$ ,  $m/z = 134$  belonged to  $\text{C}_9\text{H}_{11}\text{N}$ , and  $m/z = 120$  belonged to  $\text{C}_8\text{H}_9\text{N}$ . This is because relative abundance and fragmentation pattern demand that these fragments belong to them.

Table 1. FTIR spectral data (wave number)  $\text{cm}^{-1}$  of ligand and its complexes.

Compound	Unique ( $\nu$ )	$\nu_{\text{ar}}(\text{C-H})$	$\nu_{\text{ali}}(\text{C-H})$	$\nu_{\text{ar}}(\text{C=C})$	$\nu(\text{N-CS}_2)$	$\delta(\text{CH}_2)$	$\nu(\text{C-N})$	$\nu_{\text{as,s}}(\text{CS}_2)$	N(M-S)
Schiff base	$\nu(\text{C=N})$ 1516	3059			--		1076	--	--
Secondary amine	$\nu(\text{N-H})$ 3286				--			--	--
Ligand (L)		3035	2958	1604	1492	1438	1315	1150-970	--
$[\text{Mn}(\text{L})(\text{H}_2\text{O})_2]_2$	Broad	3043, 3001	2978, 2951	1604	1448	1446	1295	1150-1005	460
$[\text{Fe}(\text{L})_2]$		3043, 3016	2951, 2897	1604	1482	1450	1270	1104-930	440
$[\text{Co}(\text{L})_2]$		3082	2943, 2885	1604	1482	1442	1360	1148-993	429
$[\text{Ni}(\text{L})(\text{H}_2\text{O})_2]_2^*$	$\nu(\text{O-H})$	3051	2958, 2897	1604	1482	1446	1309	1152-997	438
$[\text{Cu}(\text{L})(\text{H}_2\text{O})_2]_2$	$\nu(\text{O-H})$	3047, 3005	2951	1604, 1554	1486	1438	1355	1179-959	449
$[\text{Zn}(\text{L})_2]$		3039	2997, 2978	1612	1486	1450	1366	1189-999	451

*Mass spectrum of secondary amine.* The electrospray (+) mass spectrum of a secondary amine exhibited a dominant ion peak ( $\text{C}_{16}\text{H}_{20}\text{N}_2\text{O}_2$ ), (M)<sup>+</sup> at  $m/z = 272.1$ , indicating the presence of the parent basic ion. Several pieces associated with the structure of secondary amines are observable. The molecular ion has a mass-to-charge ratio of 256 due to chemical formula  $\text{C}_{16}\text{H}_{20}\text{N}_2\text{O}$  and had a mass-to-charge ratio ( $m/z$ ) of 236. The compound with the molecular formula  $\text{C}_{16}\text{H}_{16}\text{N}_2$  has a mass-to-charge ratio ( $m/z$ ) of 212.3 for the compound  $\text{C}_{14}\text{H}_{16}\text{N}_2$ , but the  $m/z$  value of 136 corresponds to the compound  $\text{C}_8\text{H}_{12}\text{N}_2$ .

*Mass spectrum of free ligand.* The electrospray (+) mass spectrum of the ligand [L] shows a sequence of fragments that are associated with the ligand. The ligand's parent ion peak is observed at  $m/z = 498$ , which corresponds to the sum of the molecular weight and the percentage composition of the compound  $\text{C}_{18}\text{H}_{17}\text{K}_2\text{N}_2\text{O}_2\text{S}_4$ . Additionally, there are other fragments detected at  $m/z = 466$ , which can be attributed to the compound  $\text{C}_{18}\text{H}_{16}\text{K}_2\text{N}_2\text{S}_4$ . Another fragment at  $m/z = 344$  is associated with the compound  $\text{C}_{11}\text{H}_{17}\text{KN}_2\text{S}_4$ , while  $m/z = 272.13$  corresponds to the compound  $\text{C}_8\text{H}_{13}\text{KN}_2\text{S}_3$ . Lastly, the fragment at  $m/z = 256.4$  is attributed to the compound  $\text{C}_7\text{H}_9\text{KN}_2\text{S}_3$ .

#### UV-Vis spectral and magnetic moment measurements

The ligand and its complexes were analyzed using UV-Vis spectroscopy, with DMSO serving as the solvent and reference. The ligand exhibits absorption at 230 nm, attributed to ( $\pi \rightarrow \pi^*$ ) and at 291 nm, attributed to ( $n \rightarrow \pi^*$ ) [21]. Regarding the electronic spectra, the produced compounds exhibited absorption bands within the range of 260-322 nm, which are associated with intra-ligand transitions. The presence of bands at around 400 nm indicates the occurrence of charge transfer (M-L) between the metal and the ligand, providing evidence for the development of the complexes. The  $\text{Mn}^{\text{II}}$  d-d transitions exhibit peaks at 412 nm, known as  ${}^6\text{A}_{1g} \rightarrow {}^4\text{T}_{1g}({}_{4G})$ , and 741 nm, known as  ${}^6\text{A}_{1g} \rightarrow {}^4\text{E}_g, {}^4\text{T}_{1g}({}_{4P})$ . The effective magnetic moment value of  $\mu_{\text{eff}}$  is 1.33 B.M., indicating the presence of a deformed octahedral structure around the core atoms [22]. The  $\text{Fe}^{\text{II}}$  complex exhibited an absorption peak at 559 nm, indicating an electronic transition of the d-d type known as the  ${}^5\text{E}_g \rightarrow {}^5\text{T}_{2g}$  transition. The complicated tetrahedral structure of the complex was a result of this change throughout development. The electronic spectra [23] indicate that the

effective magnetic moment ( $\mu_{\text{eff}}$ ) is 5.20 B.M. This validates the hypothesis. The  $\text{Co}^{\text{II}}$  complex exhibited a maximum intensity at 633 nm while undergoing the transition from  ${}^4\text{A}_{2\text{g}(\text{F})}$  to  ${}^4\text{T}_{1\text{g}(\text{P})}$ . The change occurred precisely at this moment. This transition was accompanied by a tetrahedral form. The Co atom structure in a tetrahedral arrangement results in an effective magnetic moment of 4.67 B.M. ( $\mu_{\text{eff}}$ ) [23]. The transition from  ${}^3\text{A}_{2\text{g}}$  to  ${}^3\text{T}_{1\text{g}(\text{P})}$  in  $\text{Ni}^{\text{II}}$  exhibited a peak at 440 nm. This summit signifies the transition. The presence of a peak at 559 nm signifies the transition from the  ${}^3\text{A}_{2\text{g}}$  state to the  ${}^3\text{T}_{1\text{g}(\text{F})}$  state. This transition started with the introduction of tetrahedrons. Reference [24] establishes a correlation between the tetrahedral structure of the  $\text{Ni}^{\text{II}}$  complex and its magnetic moment value ( $\mu_{\text{eff}} = 3.18$  B.M.). The  $\text{Cu}^{\text{II}}$  molecule exhibited a peak absorption at 741 nm, suggesting a transition from  ${}^2\text{E}_{\text{g}}$  to  ${}^2\text{T}_{2\text{g}}$  energy levels. The change was activated by the complex's complicated octahedral structure [22]. The magnetic moment value  $\mu_{\text{eff}}$  of 1.9 B.M. for the  $\text{Cu}^{\text{II}}$ -complex, as well as this value agreement with structures geometry [25]. As for the  $\text{Zn}^{\text{II}}$  complex, a peak not appeared (d-d) transition because it has  $d^{10}$  orbital, therefore attributed to the tetrahedral shape [21]. The magnetic moment value  $\mu_{\text{eff}}$  of 0.00 B.M for the  $\text{Zn}^{\text{II}}$  complex, diamagnetic properties  $d^{10}$ , as for as normally prefer tetrahedral coordination [26].

#### *${}^1\text{H}$ -NMR for ligand and its Zn-complex*

The peak with the maximum intensity in the  ${}^1\text{H}$ -NMR spectra of the ligand corresponded to the  ${}^1\text{H}$  proton of the hydroxyl group (OH), with a chemical shift of 13.38 ppm. The peak between  $\delta = 6.55$  and  $\delta = 7.14$  ppm was attributed to the aromatic ring protons ( $\text{H}_{2,2'}$ ,  $\text{H}_{3,3'}$ ,  $\text{H}_{4,4'}$  and  $\text{H}_{6,6'}$ ). The  $\text{H}_{8,8'}$ -position in the methylene group, is responsible for the peak that is seen at  $\delta = 4.25$  ppm. The proton  $\text{H}_{7,7'}$  belonging to the aliphatic group is responsible for the apparent peak situated at  $\delta = 3.77$  ppm. One may attribute the apparent signal at  $\delta = 3.22$  ppm to the water that is present in the residue. As seen in Figure 1, the peak that occurred at  $\delta = 2.50$  ppm was a reference to the protons that were present in the DMSO.

Taking into consideration the zinc complex, a peak was seen at  $\delta = 9.66$  ppm, which was attributed to the  ${}^1\text{H}$  proton of the hydroxyl group (OH). It has been determined that the aromatic ring protons  $\text{H}_{2,2'}$ ,  $\text{H}_{3,3'}$ ,  $\text{H}_{4,4'}$ , and  $\text{H}_{6,6'}$  are responsible for the apparent peaks that occur between  $\delta = 6.78$  and  $\delta = 7.12$  ppm. When the apparent peak is measured at  $\delta = 5.03$  ppm, it is determined the  $\text{H}_{7,7'}$  proton is located position in the methylene group. Figure 2 illustrates that the peaks at  $\delta = 3.94$  ppm, which correspond to the  $\text{H}_{8,8'}$  proton of the aliphatic group,  $\delta = 3.35$  ppm, which corresponds to the residue of water, and  $\delta = 2.51$  ppm, which corresponds to the protons of the DMSO had been assigned to them. This comparison is made between the peaks that are displaced downfield and those that are found in the ligand. Possible explanations for this phenomenon include the presence of metals that have electron-withdrawing groups ( $\text{CS}^{2-}$ ).

#### *${}^{13}\text{C}$ -NMR spectrum for ligand and its Zn-complex*

The ligand's  ${}^{13}\text{C}$ -NMR spectra exhibited a peak at a chemical shift of  $\delta = 206.90$  ppm, which was attributed to the  $\text{C}_{9,9'}$  atoms in the  $\text{NCS}_2$  group. The carbon atoms in the aromatic ring were attributed to the peaks ranging for  $\text{C}_{1,1'}$  and  $\text{C}_{5,5'}$  correspond to  $\delta = 147.15$  and  $\delta = 153.96$  ppm, respectively. The other aromatic peaks corresponded to  $\text{C}_{2,2'}$ ,  $\text{C}_{3,3'}$ ,  $\text{C}_{4,4'}$ , and  $\text{C}_{6,6'}$  appear between  $\delta = 110$ -125 ppm. The peaks are located at  $\delta = 53.30$  ppm, which are ascribed to the  $\text{C}_{8,8'}$  atoms in the aliphatic group. The peaks at  $\delta = 48.10$  ppm are assigned to the  $\text{C}_{7,7'}$  atoms in the methylene group at the  $7,7'$ - position. Lastly, the peaks at  $\delta = 42.49$  ppm are assigned to the DMSO [29]. This chemical shift for  $\text{C}_{9,9'}$  supported by its complicated form, seen at the  $\delta = 195$  ppm in Figure 4, which was ascribed atoms in the  $\text{NCS}_2$  group. The peaks ranging for  $\text{C}_{1,1'}$  and  $\text{C}_{5,5'}$  combined in complex correspond to  $\delta = 148$  ppm correspond to the carbon atoms located. The other aromatic ring, namely for  $\text{C}_{2,2'}$ ,  $\text{C}_{3,3'}$ ,  $\text{C}_{4,4'}$ , and  $\text{C}_{6,6'}$  due to chemical shifts at  $\delta = 110.75$ -125 ppm. Moreover the  $\text{C}_{8,8'}$  atoms in the aliphatic group due to  $\delta = 57$  ppm,

whereas the chemical shifts at  $\delta = 54.92$  ppm correspond to the C7,7' atoms in the methylene group. The point at chemical shifted  $\delta = 43.50$  ppm is attributed to the solvent DMSO [27], as seen in Figure 4.

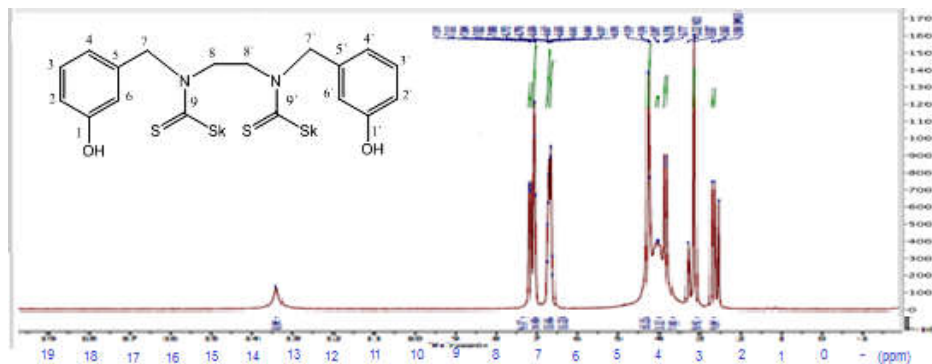


Figure 1.  $^1\text{H-NMR}$  proton spectrum of the salt ligand.

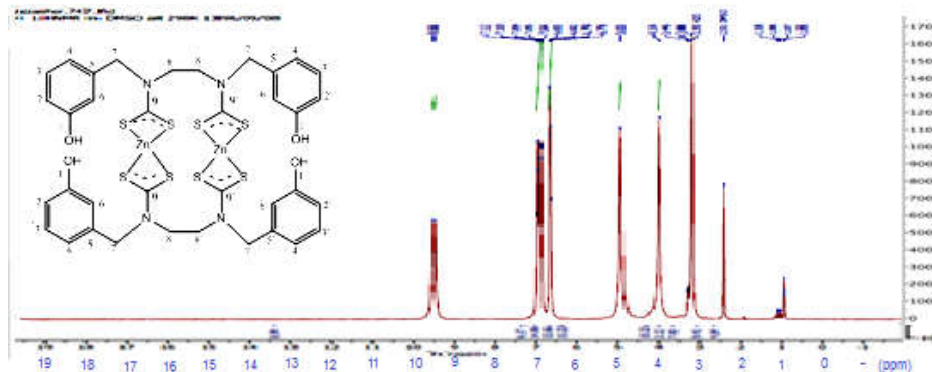


Figure 2.  $^1\text{H-NMR}$  proton spectrum of the zinc complex.

#### *Atomic absorption to capture heavy elements*

Immediately after the addition of the ligand, an investigation of the atomic absorption of water that included components of iron and copper was carried out. Before the addition of the ligand, the concentration of iron was 29.9940 mg/L; however, after the addition of the ligand, the concentration of iron dropped to 0.4098 mg/L. Taking into account the concentration of copper, it dropped to 0.2000 mg/L, which is a significant reduction from the 5.5500 mg/L that it was before the ligand was added. As a result, the equation that was described indicated that the percentage of iron capture was (98%) and the percentage of copper capture was (96%). This was a clear evidence that the ligand that was generated had the ability to grab metallic elements and form complexes [28].



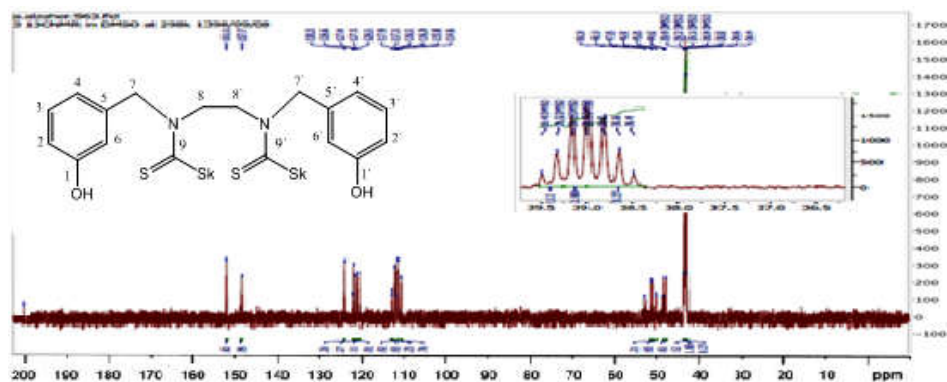


Figure 3. The  $^{13}\text{C}$ -NMR proton spectrum of the salt ligand.

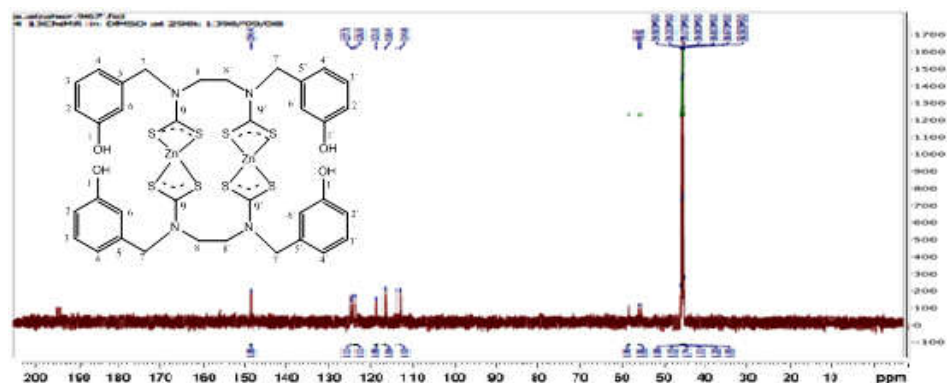


Figure 4. The  $^{13}\text{C}$ -NMR proton spectrum of the zinc complex.

## CONCLUSION

Through the preparation and characterization of the ligand and its interaction with metal ions, as well as the verification of the stereoscopic shape of the resultant complexes using physical and chemical measures, it was determined that two distinct structural forms were observed: tetrahedral and octahedral. The presence of scavenging heavy metal ions ( $\text{Fe}^{\text{II}}$  and  $\text{Cu}^{\text{II}}$ ) in the western water at concentrations of 98% and 96%, respectively resulted in the formation of these stable structures.

## REFERENCES

1. Hamooda, E.S.; Al-Fahdawi, A.S. Application of salicylaldehyde based-metal binuclear dithiocarbamate complexes for iron and copper removal from wastewater. In IOP Conference Series: *Materials Science and Engineering* **2021**, 1058, 012083.
2. Tiekink, E.R.T. On the coordination role of pyridyl-nitrogen in the structural chemistry of pyridyl-substituted dithiocarbamate ligands. *Crystals* **2021**, 11, 286.

3. Motaung, M.P.; Adeyemi, J.O.; Smida, Y.B.; Ferjani, H.; Kabanda, M.M.; Onwudiwe, D.C.; Hosten, E. Synthesis, structural, and DFT studies of Cu(II) dithiocarbamate complexes. *J. Mol. Struct.* **2023**, 1271, 133988.
4. Sarker, J.C.; Hogarth, G. Dithiocarbamate complexes as single source precursors to nanoscale binary, ternary and quaternary metal sulfides. *Chem. Rev.* **2021** 121, 6057-6123.
5. Ratia, C.; Ballén, V.; Gabasa, Y.; Soengas, R.G.; Velasco-de Andrés, M.; Iglesias, M.J.; Soto, S.M. Novel gold(III)-dithiocarbamate complex targeting bacterial thioredoxin reductase: Antimicrobial activity, synergy, toxicity, and mechanistic insights. *Front. Microbiol.* **2023**, 14, 1198473.
6. Moghadam, M.E.; Rezaeisadat, M.; Mansouri-Torshizi, H.; Hosseinzadeh, S.; Daneshyar, H. New anticancer potential Pt complex with tertamyl dithiocarbamate ligand: Synthesis, DNA targeting behavior, molecular dynamic, and biological activity. *J. Mol. Liq.* **2023**, 379, 121651.
7. Yeo, C.I.; Tiekink, E.R.T.; Chew, J. Insights into the antimicrobial potential of dithiocarbamate anions and metal-based species. *Inorganics* **2021**, 9, 48.
8. Ajibade, P.A.; Idemudia, O.G.; Okoh, A.I. Synthesis, characterization and antibacterial studies of metal complexes of sulfadiazine with N-alkyl-N-phenyldithiocarbamate. *Bull. Chem. Soc. Ethiop.* **2013**, 27, 77-84.
9. Pratt, M.D.; Beer, P.D. Heterodinuclear ruthenium(II) bipyridyl-transition metal dithiocarbamate macrocycles for anion recognition and sensing. *Tetrahedron Lett.* **2004**, 60, 11227-11238.
10. Ibrahim, A.B.; Farh, M.K.; Santos, I.C.; Paulo, A. Nickel complexes bearing snn and ss donor atom ligands: Synthesis, structural characterization and biological activity. *Appl. Organomet. Chem.* **2019**, 33, e5088.
11. Alsalihi, I.I.; Al-khafaji, Y.F.; Al-fahdawi, A.S.; Atiyah, E.M. Synthesis and characterization of benzil crown cyclic Schiff base ligand and its metal complexes. *Bull. Chem. Soc. Ethiop.* **2022**, 36, 791-799.
12. Al-Jiboury, M.M.; Al-Nama, K.S. Preparation, characterization and biological activities of some unsymmetrical Schiff bases derived from *m*-phenylenediamine and their metal complexes. *Raf. J. Sci.* **2019**, 28, 23-36.
13. Alfahdawi, A.S.; Al-Sorchee, S.M.; Saleh, S.E.; Saleh, M.M. Synthesis and study of N,N-(ethane-1,2-diyl) bis(1-phenyl methanimine) and their complex derivative with in-vivo and in-vitro bacterial biological study. *Egypt. J. Chem.* **2021**, 64, 2879-2888.
14. Al-Fahdawi, A.S.; Al-Kafajy, H.A.; Al-Jeboori, M.J.; Potgieter, H. New bimetallic bisdithiocarbamate-based macrocyclic complexes; Preparation and spectral characterization. *Chem. Express* **2014**, 4, 267-262.
15. Jawale, V.; Al-fahdawi, A.; Salve, S.; Pandit, S.; Dawange, G.; Gugale, G.; Chaskar, M.; Hammiche, D.; Arbuj, S.; Pandit, V. 6, 13-pentacenequinone/zinc oxide nanocomposites for organic dye degradation. *Mater Today Proc.* **2022**, 52, 17-20.
16. Hasan, H.A.; Yousif, E.I.; Al-Jeboori, M.J. Metal-assisted assembly of dinuclear metal(II) dithiocarbamate Schiff-base macrocyclic complexes: Synthesis and biological studies. *Global J. Inorg. Chem.* **2012**, 3, 1-7.
17. Beniwal, S.; Kumar, A.; Chhimpia, S.; Rai, J.; John, P.J.; Singh, Y.; Sharma, J. Synthesis and characterization of antimony(III) heteroleptic derivatives having oxygen, nitrogen and sulfur containing organic moieties with their antibacterial and antioxidant activities. *Phosphorus Sulfur, Silicon Relat. Elem.* **2019**, 1949, 1-8.
18. Saad, S.T. Co(II) and Ni(II) complexes with bis(4-((E)-(4,5-diphenyl-1H-imidazol-2-yl) diazenyl) phenyl) methane: Synthesis, characterization and anti-corrosion effect investigation. *Bull. Chem. Soc. Ethiop.* **2024**, 38, 963-971.
19. Fayad, N.K.; Al-Noor, T.H.; Mahmood, A.A.; Malih, I.K. Synthesis, characterization, and antibacterial studies of Mn(II), Fe(II), Co(II), Ni(II), Cu(II) and Cd(II) mixed-ligand

- complexes containing amino acid (L-valine) and (1,10-phenanthroline). *Synthesis* **2013**, 3, 66-73.
20. Khalil, M.H.; Abdullah, F.O. Synthesis, characterisation, and anticancer and antioxidant activities of novel complexes of palladium and an organic Schiff-base ligand. *Bull. Chem. Soc. Ethiop.* **2024**, 383, 605-613.
  21. Al-Mohammadi, N.A.H.A.; Al-Fahdawi, A.S.; Al-Janabi, S.S. Design and characterization of new dinuclear macrocyclic dithiocarbamate complexes by the preparation of a free ligand derived from isopropylamine. *Iraqi J. Sci.* **2021**, 62, 1-15.
  22. Trávníček, Z.; Pastorek, R.; Slovák, V. Novel octahedral nickel(II) dithiocarbamates with bi- or tetradentate N-donor ligands: X-ray structures of [Ni(Bzppzdtc)(phen)<sub>2</sub>]ClO<sub>4</sub>·CHCl<sub>3</sub> and [Ni(Bz<sub>2</sub>dtc)<sub>2</sub>(cyclam)]. *Polyhedron* **2008**, 27, 411-419.
  23. Chantrell, R.W.; O'Grady, K. Magnetic moments. *Tech. Phys.* **1984**, 15, 103.
  24. Alshdoukhi, I.F.; Al-barwari, A.S.; Aziz, N.M.; Khalil, T.; Faihan, A.S.; Al-Jibori, S.A.; Al-Janabi, A.S. Pd(II), Pt(II), Zn(II), Cd(II) and Hg(II) complexes of the newly prepared 1,2-benzo-isothiazol-3-(2H)-dithiocarbamate (BIT-DTC) ligand. *Bull. Chem. Soc. Ethiop.* **2024**, 38, 889-899.
  25. Al-Nassiry, A.I.; Al-Janabi, A.S.; Thayee Al-Janabi, O.Y.; Spearman, P.; Alheety, M.A. Novel dithiocarbamate–Hg(II) complexes containing mixed ligands: synthesis, spectroscopic characterization, and H<sub>2</sub> storage capacity. *J. Chin. Chem. Soc.-Taip.* **2020**, 67, 775-781.
  26. Karimi, M.; Amani, V.; Aboufazel, F.; Lotfi Zadeh Zhad, H.R.; Sadeghi, O.; Najafi, E. Flame atomic absorption determination of gold ion in aqueous samples after preconcentration using 9-acridinylamine functionalized  $\gamma$ -alumina nanoparticles. *J. Chem.* **2013**, 2013, 142845.
  27. Stala, Ł.; Ulatowska, J.; Polowczyk, I. A review of polyampholytic ion scavengers for toxic metal ion removal from aqueous systems. *Water Res.* **2021**, 203, 117523.
  28. Han, R.; Zou, W.; Li, H.; Li, Y.; Shi, J. Copper(II) and lead(II) removal from aqueous solution in fixed-bed columns by manganese oxide coated zeolite. *J. Hazard. Mater.* **2006**, 137, 934-942.